Journal of Environmental Chemical Engineering 13 (2025) 117568

Contents lists available at ScienceDirect

Journal of Environmental Chemical Engineering

journal homepage: www.elsevier.com/locate/jece

Multi-year trends in the spatiotemporal occurrence and fate of naphthenic acid fraction compounds in a pilot-scale engineered treatment wetland

Ian Vander Meulen [a,b], Jason M.E. Ahad [c], Christine Martineau [d], Douglas G. Muench [e], Dena W. McMartin [a,f,*], John V. Headley [b]

[a] Department of Civil, Geological and Environmental Engineering, University of Saskatchewan, 57 Campus Drive, Saskatoon, SK, Canada
[b] Watershed Hydrology & Ecology Research Division, Environment and Climate Change Canada, National Hydrology Research Centre, 11 Innovation Blvd, Saskatoon, SK, Canada
[c] Geological Survey of Canada, Natural Resources Canada, Québec, QC, Canada
[d] Laurentian Forestry Centre, Natural Resources Canada, 1005 Rue du Peps, Québec, QC, Canada
[e] Department of Biological Sciences, University of Calgary, 2500 University Drive NW, Calgary, AB, Canada
[f] Department of Geography and Environment, University of Lethbridge, 4401 University Drive, Lethbridge, AB, Canada

ARTICLE INFO

Keywords:
Naphthenic acid fraction compounds
Athabasca Oilsands
Pilot-scale wetlands
Engineered wetlands
Tailings pond water reclamation
Orbitrap-MS analysis

ABSTRACT

In the Athabasca Oil Sands region (AOSR) of Alberta, Canada, there are ~1.4 billion m^3 of fluid tailings containing known toxic constituents which will require treatment and must be reclaimed before closure. One class of contaminants of concern are naphthenic acid fraction compounds (NAFCs). While various treatment strategies have been considered, constructed wetland treatment systems (CWTSs) have emerged as a semi-passive, high throughput, and potentially cost-effective option. Here, non-targeted Orbitrap high-resolution mass spectrometry was applied to assess the NAFC remediation efficacy of a 1-ha CWTS operated over two field seasons (2021 and 2022) at a site situated in the Northern of Alberta. Concentrations of total NAFCs decreased consistently during a closed CWTS operation with OSPW recirculation at each field seasons. Concurrently, O_2-NAFCs (i.e., classical NAs) steadily decreased while more-oxygen-rich formulae increased in spectral abundance, consistent with oxidative degradation. Attenuation rates of NAFCs were more rapid at the outset of the season (~0.53 mg/L/d), where treatment rates eventually decreased (~0.25 mg/L/d). Molecular-level characterization of treatment outcomes showed that the highest molecular weight O_2-NAFCs detected (i.e., #C > 14) decreased the most, whereas all O_3- and O_4-NAFCs generally increased in relative spectral abundance. Shallow, heavily vegetated cells of the wetlands tended to have lower NAFC concentrations and more oxygen-rich compounds, suggesting substantial attenuation of NAFCs in these segments. These results demonstrate that this field-scale CWTS effectively in depletes and transforms OSPW-derived NAFCs under environmental conditions found in the AOSR

1. Introduction

The Athabasca Oil Sands Region (AOSR) of Alberta, Canada has one of the world's largest identified petroleum reserves at an estimated 1.7 trillion barrels-of-oil-equivalent, of which ~315 billion are recoverable [3]. This extensive bitumen deposit has commensurate large-scale mining operations, which depend on water-based extraction protocols. Mines operating in the AOSR use modified versions of the Clark hot water extraction process to strip bitumen from oil sands ore [20], which has historically required 2–4 barrels of fresh water from the Athabasca River for every barrel of bitumen produced [2]. As higher volumes of oil sands process-affected water (OSPW) accumulate, some constituents can concentrate to levels that are toxic to various organisms [41,42]. As of 2024, there are no water release guidelines for OSPW or agreements on treatment technologies, instead requiring that operators retain OSPW on-site until further direction can be given. Owing to these factors and a long history of oil production in the region, the total volume of fluid tailings in the AOSR is approximately 1.4 billion m^3, of which approximately 400 million m^3 is OSPW [4].

The OSPW present in the AOSR is a complex mixture of water, salts, unrecovered hydrocarbons, sand, fine clay, and residual greases [36]. Despite the considerable complexity of OSPW, naphthenic acids (NAs) [35,47] and related naphthenic acid fraction compounds (NAFCs) [11,12,32,63] have been consistently implicated as some of the primary

* Corresponding author at: Department of Civil, Geological and Environmental Engineering, University of Saskatchewan, 57 Campus Drive, Saskatoon, SK, Canada.
E-mail address: Dena.mcmartin@uleth.ca (D.W. McMartin).

https://doi.org/10.1016/j.jece.2025.117568
Received 24 March 2025; Received in revised form 4 June 2025; Accepted 11 June 2025
Available online 12 June 2025

bitumen-derived aquatic toxicants of concern. The class of compounds described by the term NAs includes those aliphatic hydrocarbons adhering to the general formula $C_nH_{2n+Z}O_2$, where Z is a negative, even integer describing the degree of unsaturation (i.e., number of aliphatic intramolecular bonds) in a given compound [14]. The compound class described by the term NAFCs is broader, encompassing NAs, as well as technically non-naphthenic formulae (e.g., aromatic compounds) as well as those containing a broader variety of heteroatoms (i.e., atoms other than carbon or hydrogen, e.g., S, N, and O_x where x ≈ 1–10) [30,32,61]. This class of compounds are potentially toxic to a variety of organisms, including various fishes [31,54], invertebrates [10], and mammals [51]. While there has been a focus on characterizing the occurrence of NAFCs in the Athabasca oil sands [52,58,62], these compounds can occur wherever degraded petroleum might be present [26,53,65].

There are a variety of different and complementary treatment technologies that have been evaluated for treatment of NAFCs, including the use of sorbents [45,68], chemically oxidative treatments [44,67], photocatalysts [22,39,43], and constructed wetland treatment systems (CWTSs) [1,18,6,59,66,8]. While each treatment approach has particular pros and cons, the CWTS strategy is advantageous for its relatively low ongoing cost and little need for ongoing energy and chemical inputs, and the potential of CWTSs to treat large volumes of wastewater. Further, treatment wetlands have been applied as a strategy for contaminant management in the contexts of municipal [16,38] and industrial [23,57] wastewaters, demonstrating the robustness of the approach for a variety of issues.

A previous study measured the degradation of classical NAs in a field-scale treatment wetland [18], but none currently report on the broader suite of NAFCs therein. Attempting to replicate greenhouse-scale NAFC attenuation results in a pilot-scale system, this study reports the progression of NAFC transformation and attenuation in a 1-ha scale field-pilot CWTS on the Kearl Oil Sands site located in Northern Alberta, as substantiated by non-targeted Orbitrap mass spectrometry over two field sampling seasons. The primary objective in this work would be to validate the extent(s) to which results observed in lab-scale CWTSs [1,56,59] translate to a pilot-scale field-CWTS with respect to elimination and oxidation of NAFCs. For the first time, we provide quantitative estimates of empirically derived NAFC elimination rates over an extended monitoring period and provide evidence for selective attenuation at the molecular level.

2. Methods and materials

2.1. Wetland operation and flow regime

The Kearl Treatment Wetland (KTW) was constructed as a contained, recirculating free water surface- wetland system (Fig. 1), where an open water column circulates end-to-end above added growth substrates (i.e., sediments) supporting the growth of aquatic microorganisms (e.g., algae and biofilms) and rooting of macrophytes [18,17]. This pilot wetland is unique and cannot be replicated as a whole or compared for various reasons (e.g., cost, space, operations considerations, etc.), but provides a unique opportunity to assess NAFC remediation under near-operational conditions in a wetland design that incorporates both deep and shallow segments. The wetland is 0.76 ha in surface area and 6400–10,800 m of OSPW between all cells when filled to capacity, where exact volumes vary. The wetland was consistently filled in the forebay area (Table 1), which is physically closest to nearby tailings and OSPW impoundment infrastructure. In 2021 the wetland was filled to 6391 m; in 2022 the wetland was filled to 10,791 m; in 2024 the wetland was filled to 8772 m. The wetland has been operated with a targeted retention time of 14 d at each field season, pumping at approximately 5 L/s. After each season of operation, the injected water in the wetland is drained and residual OSPW removed as best as possible. The approximate coordinates, surface areas, and engineered depths of all cells are listed in

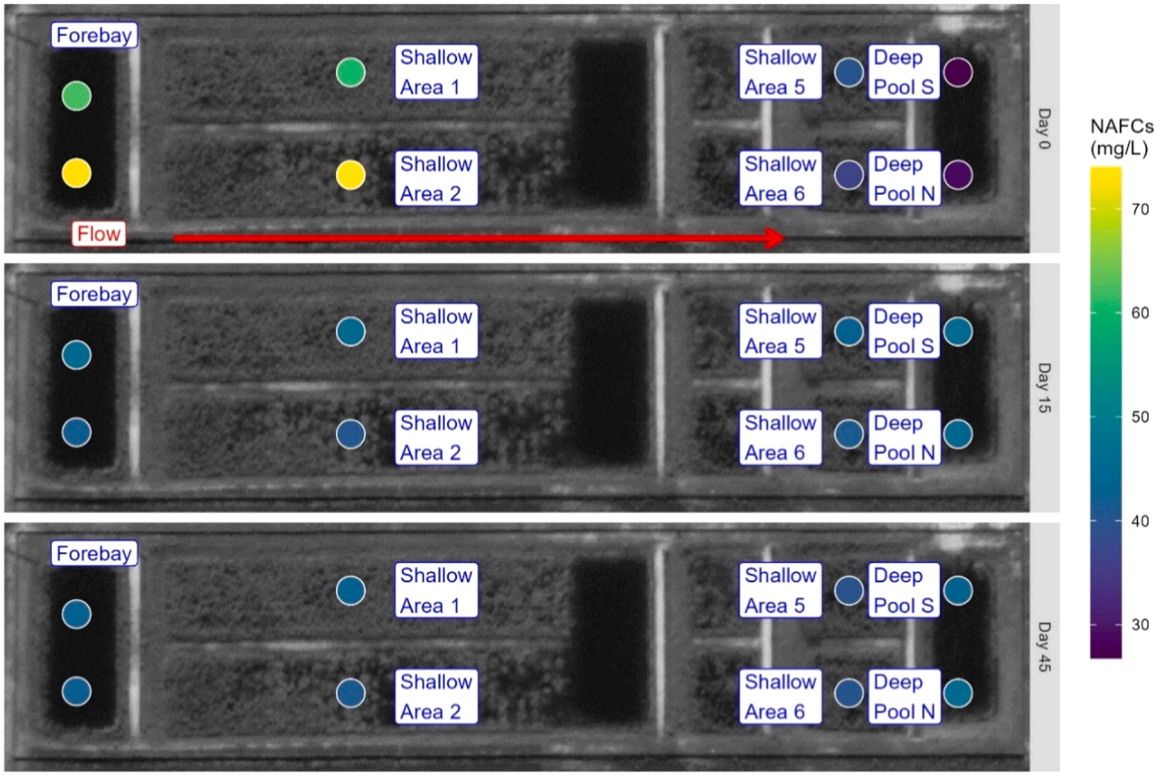

Fig. 1. Concentrations of NAFCs detected over 45 days of Kearl CWTS operation during the 2021 field season superimposed over an aerial photo of the site turned 180° (e.g., south is upwards) where flow is east to west (oriented left-to-right). The underlying image was taken from Google Earth Pro ("[28]) from coordinates at approximately 57.438280° latitude and −111.146230° longitude.

Table 1
Locations, approximate surface areas, and depths of sampling locations in the Kearl constructed treatment wetland.

Wetland Cell	Latitude	Longitude	Surface Area (m^2)	Depth (m)
Forebay area	57.43821	−111.144218	125	1.7
Shallow Area 1	57.438151	−111.145634	275	0.4
Shallow Area 2	57.438364	−111.145634	275	0.4
Deep Pool 1	57.43821	−111.146747	135	1.7
Shallow Area 5	57.438151	−111.147874	100	0.4
Shallow Area 6	57.438364	−111.147874	100	0.4
Deep Pool 2	57.43821	−111.148432	125	1.7

Table 1.

For 2021 season, the initial OSPW fill period started on May 30, 2021, and the wetland was operated normally until warm weather (e.g., average of 29.3 ± 6.3 °C for a high over days 23–45) in the region resulted in low water levels from evapotranspiration and wetland flow was terminated (July 14, 2021; 45 days). Over the duration of the 2021 season, regional temperatures ranged between nighttime lows of 13.6 ± 4.4 °C and daytime highs of 25.7 ± 6.5 °C, with daylight length ranging from 15 h 31 min (May) to 18 h (June). In the 2022 field season, the wetland was filled on June 13, 2022, but was topped up with further additions of OSPW on July 8 (day 20) and August 27, 2022 (day 70), with approximately 1545 m and 1290 m respectively to compensate for water loss from the system due to evapotranspiration. Over the duration of the 2022 season, regional temperatures ranged between nighttime lows of 11.6 ± 3°C and daytime highs of 23.7 ± 4.4 °C, with daylight length ranging from 18 h (June) to 12 h (September). Although there was not weather monitoring happening on-site, data from the Mildred Lake weather station are used here as a proxy [29]. Mean daily solar insolation for a flat surface at a comparable latitude (Fort MacKay) ranges between 11.7 and 12.9 kWh/m^2 between May to September [48].

2.2. Sample collection and extraction for total naphthenic acid fraction compounds

Sampling was carried out in an attempt to capture temporal differences in mixture chemistry that emerged with increasing OSPW residence time in the CWTS. Owing to differences in contractor availability, sampling regimes were adjusted between field seasons; single samples were collected from each cell listed in Table 1 during each sampling event in 2021, and duplicate samples were collected during each event in 2022. Grab samples from each of the CWTS wetland cells were collected in pre-cleaned 1 L amber glass bottles with PTFE closures, and immediately put into wet ice and stored at < 4 °C until shipment (< 1 week). Samples were sent to the National Hydrology Research Centre in Saskatoon, Saskatchewan at < 4 °C and prepared according to the procedure originally described by Headley et al. [33] for quantification and characterization of NAFCs. In summary, sample volumes of ~100 mL were measured and exact volumes were recorded. Prior to extraction, 200 mg Biotage ENV+ SPE cartridges (6 mL) were sequentially rinsed with separate washes of 6 mL of MilliQ water, 6 mL of LC/MS-grade methanol (Fisher Scientific, Edmonton, AB, Canada), and reconditioned with a further 6.0 mL of MilliQ water. After the column rinsing and conditioning steps were complete, samples were acidified to pH < 2 with formic acid (> 98 % purity; Fisher Scientific, Edmonton, AB, Canada), then immediately transferred through polytetrafluoroethylene (PTFE) transfer lines to conditioned SPE cartridges at 3–5 mL/min. Following complete sample extraction, cartridges were de-salted by rinsing with 6 mL of MilliQ water. Rinsed SPE cartridges were dried completely under a gentle vacuum and NAFCs eluted in 6.0 mL of methanol under gravity to clean, dry, labelled glass culture tubes. The eluted extracts were dried down completely under a gentle flow of N_2 gas (5.0-grade high-purity; Linde Canada, Saskatoon, SK) while partially immersed in a 40 °C water bath. Dried sample extracts were reconstituted in 50:50 acetonitrile:H_2O with 0.1 % NH_4OH by vortexing for 10–15 s in the culture tube. Reconstituted sample extracts were transferred to 2.0 mL amber LC/MS autosampler vials prior to analysis. For ongoing analysis of potential lab contamination, method blanks were extracted using Milli-Q water following the same protocol. As method blanks were below 0.1 mg/L of total material, no corrections to quantitation were necessary.

2.3. Orbitrap mass spectrometry analyses

Prepared sample extracts were analyzed following a previously-reported protocol [62]. In brief, reconstituted sample extracts were placed in an Accella PAL autosampler, and 5 μL injections of each were analyzed with an LTQ Velos Elite Orbitrap Mass Spectrometer (ThermoFisher Scientific, Waltham, MA, USA) via loop injection in negative-ion mode electrospray ionization. Sample data were acquired at 240,000 resolution (as measured at *m/z* 400 by peak width at half-maximum) over a mass range from *m/z* 100 – 600, where acquired *m/z* data were recalibrated using an internal lock mass at *m/z* 212.07507- (n-butyl benzenesulfonamide) for scan-to-scan mass calibration correction. Instrument conditions were as follows: sheath gas flow rate of 25 (arbitrary units); spray voltage of 2.90 kV; an auxiliary gas flow rate of 5 (arbitrary units); the S lens radio frequency level at 67 %; heater temperature at 50°C; and capillary temperature at 275°C. The infusion solvent was 50:50 acetonitrile:water with 0.1 % ammonium hydroxide at a flow rate of 200 μL/min.

Quantification of NAFCs was achieved by analyzing samples in batches of 12 bracketed by external standard curve with standards prepared between 10 and 100 mg/L of NAFCs using an OSPW-derived extract [50] previously standardized against a commercial standard via FTIR [33]. When major water chemistry parameters were collected in 2022, the concentrations of [Cl^-] were used to prepare a linear regression for an evapotranspiration factor to apply to NAFC concentrations. Concentrations of [Cl^-] and [Na^+] were also collected in 2021, but did not reflect evaporating trends, with data reported in Table S1. Concentrations of [Cl^-] and [Na^+] in the 2022 field season are both reported in Table S2, which were reported elsewhere (Beaulieu-Laliberté et al., In prep.). This NAFC quantification method lacks standard reference materials, and so there are similar interpretational limitations for other NA and NAFC quantification methods [24,34,46,64]. Because of the semi-quantitative nature of NAFC quantification, comparison to other studies using different quantitation methods must be done with caution.

2.4. Orbitrap qualitative data treatment and analysis

Sample data from Orbitrap-MS were prepared for qualitative analyses by background subtracting data in XCalibur 2.2 software (Thermo Fisher Scientific, Waltham, MA, USA). Background-subtracted data were imported into Composer64 1.5.6 software (Sierra Analytics, Modesto, CA, USA), where a custom multi-stage assignment algorithm was applied to the mass range between *m/z* 100–500, where de-novo assignments were made for formula as follows. Allowed atom counts in pass 1 included #C 0–50, #H 0–150, #N 0–3, and #O 0–10; in pass 2 #C 0–50, #H 0–150, #O 0–3, #S 0–5; pass 3 #C 0–50, #H 0–150, #N 0–3; pass 4 #C 0–50, #H 0–150, #N 0–3, #O 0–3, #S 0–3. All assignments included in subsequent analyses were those with mass errors ≤ 3 ppm, where typical assignment success was ≥ 85 %. Assigned formula data were exported from Composer64 and compiled for later interpretation and analysis.

Assigned sample formula data were imported into R version 4.4.1 (R [21]) and organized using custom scripts written in RStudio [49]. On import, data were base-peak normalized (i.e., base peak = 100 relative abundance). Prior to principal components analysis (PCA) data were Pareto normalized [37,60] and centered, then analyzed using the built-in prcomp function (R [21]).

Spectral comparisons were carried out between Days 0 and 98 of the 2022 field season by compiling an "average spectrum" on each respective day from across all cells of the wetland. The use of different samples as pseudo-replicates was justified by the homogeneity of NAFCs across this wetland at each time point. The average spectral abundances were evaluated for normality by Shapiro-Wilk testing where < 50 % of variables were normally distributed according to a Bonferroni-adjusted p-value at 0.05. Therefore, average spectra from Day 0 were non-parametrically evaluated against the average spectra from Day 98 by Wilcoxon matched pairs signed rank testing for significantly different features, where significance was reported by evaluating Bonferroni-corrected p-values to $p < 0.05$, $p < 0.01$, or $p < 0.001$.

3. Results

3.1. 2021 field season

Concentrations of NAFCs were tracked during three sampling events in the 2021 field season and mapped out on a wetland image (Fig. 1). On day 0, the wetland was sampled immediately after filling with OSPW. Concentrations of NAFCs were location-dependent, where those wetland cells located nearest to the fill point (i.e., the forebay) had the highest measured concentrations of NAFCs (60–70 mg/L). By day 15, concentrations had stabilized to an average concentration of 43.4 ± 1.9 mg/L (±1σ), likely as a consequence of diffusion and partial transport throughout design of the CWTS. By day 45, concentrations remained similar at 42.2 ± 1.9 mg/L (1σ). A limitation of the sampling in 2021 was that major ions were not measured, and so no surrogate measure could be used to help correct for evapotranspiration. Although it is certain that substantial evapotranspiration occurred in the system (as evidenced by water levels dropping too low for recirculation pumps to function), concentrations essentially remained consistent in the aqueous phase, which may be consistent with attenuation of NAFCs therein.

To further characterize the behaviour and fate of NAFCs in the CWTS, mass spectral data were plotted with respect to the percent abundance of heteroatom types (i.e., unique atomic formula inclusions, ignoring C and H, Fig. 2). The spatial concentration heterogeneity shown on day 0 in Fig. 1 is not well-reflected in Fig. 2, where spectra are dominated by 64–70 % O_2-NAFCs (i.e., classical NAs) regardless of location. However, through day 15–45, the relative percent abundance

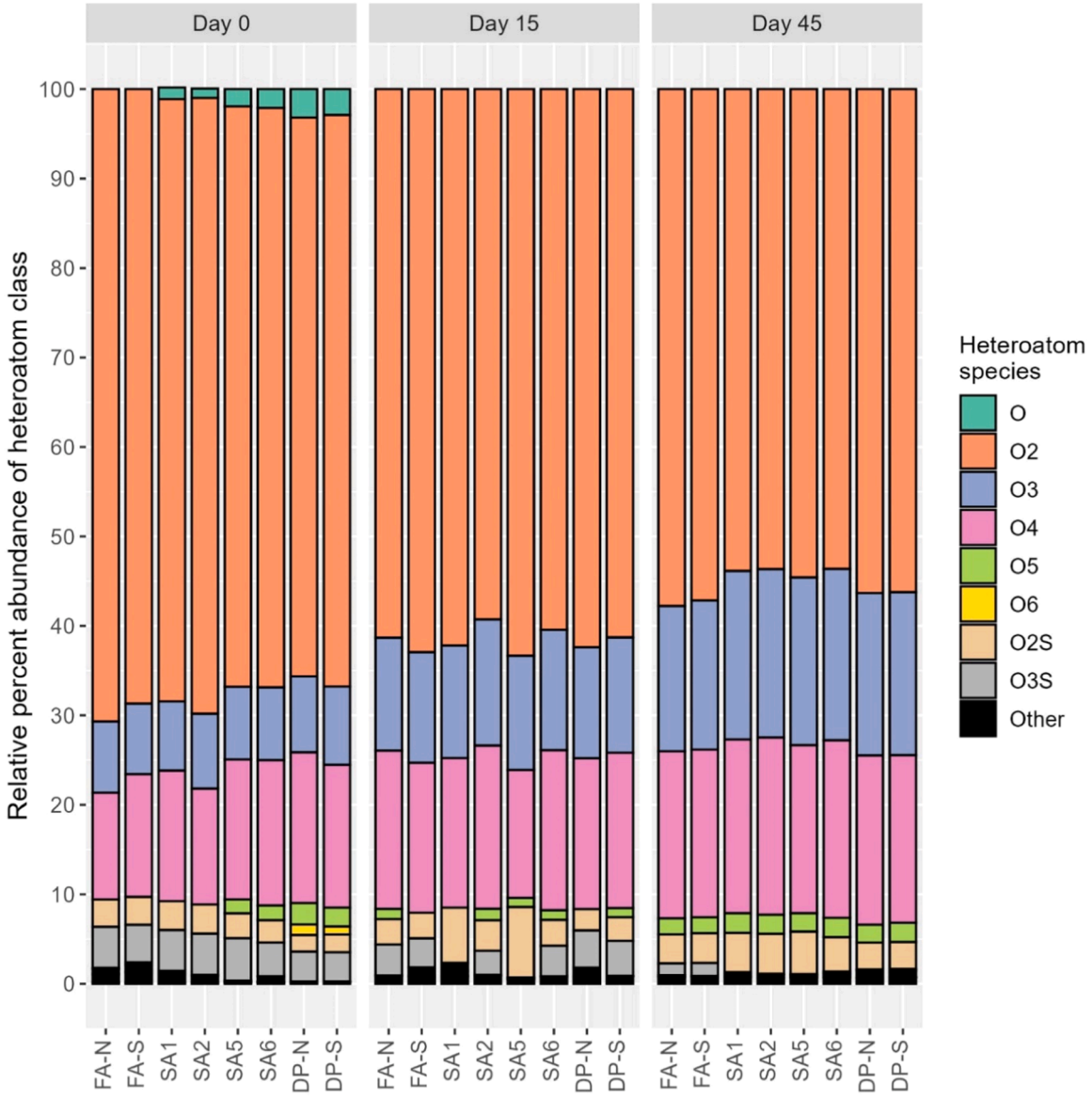

Fig. 2. A stacked bar chart communicating the percent abundance of different heteroatom formula classes (i.e., atom inclusions excluding C or H) across the 45 days of CWTS operation in the 2021 season. Sample codes refer to the Forebay Area (FA), Shallow Areas (SA), and Deep Pools (DP), which are mapped in Fig. 1.

of O_2-NAFCs decreased to 52–57 % whereas O_3- and O_4-NAFCs increased, with a small number of O_5-containing compounds appearing, consistent with oxidative reactions resulting in O_2-NAFC transformations. There is also a disappearance of O_3S-NAFCs while O_2S-NAFCs become more prevalent, which may be consistent with sulfur-reducing conditions in some pockets of the wetland where localization is likely obscured by continued intermixing.

3.2. 2022 field season

Samples were collected from the CWTS during nine separate events in 2022 before and during a 98-day growing season which extended from early summer into early autumn (May 18 to September 24, 2022). Complementary water chemistry results were also collected (Beaulieu-Laliberté et al., In prep.), allowing for calculation of a time-dependent evapotranspiration correction factor based on a linear regression of [Cl^-] over time, with concentrations thereof reported in Table S1. Prior to filling the wetland, standing water from local run-off, precipitation and possibly residual OSPW from the previous season had NAFC concentrations between 5 and 17 mg/L, depending on the wetland segment (Fig. 3). After filling of the wetland with OSPW to approximately 10,791 m, concentrations of NAFCs ranged between 57 and 72 mg/L. A sample of untreated OSPW (n = 1) had a concentration of 64 mg/L, shown at day 69 for visual separation (Fig. 3). NAFC concentrations gradually dropped throughout the treatment period, despite the addition of large relative volumes of OSPW on days 20 and 70 to replace lost water in the system (assumed lost to evapotranspiration). This drop from approximately 63.0 ± 4.7 mg/L on day 0–40.5 ± 2.7 mg/L on day 98, represents a 36 % decrease in the approximate mass of total NAFCs present from the beginning to the end of the sampling period. Very little total NAFC change was observed before and after both additions of OSPW at day 20 and day 70 (Figure S1).

Treatment rates for NAFCs in the CWTS were variable across the sampling season/experimental period, depending on whether the CWTS was operating prior to or following the first addition of OSPW. The linear regressions for each of these periods (which assumes few differences between wetland segments) is shown in Figure S2, where the sample from Deep Pool 1 North was excluded as an outlier in period 1 (i.e., day 0–15), as the difference from median concentration was greater than 5 × the median absolute deviation [40]. The slopes of the regressions differed, where the approximate rate of [Cl^-]-normalized NAFC removal was ~0.53 mg/L/ per day in period 1, whereas that rate was reduced to approximately 0.25 mg/L per day in period 2.

The 2022 CWTS was also evaluated for changes in NAFC heteroatom

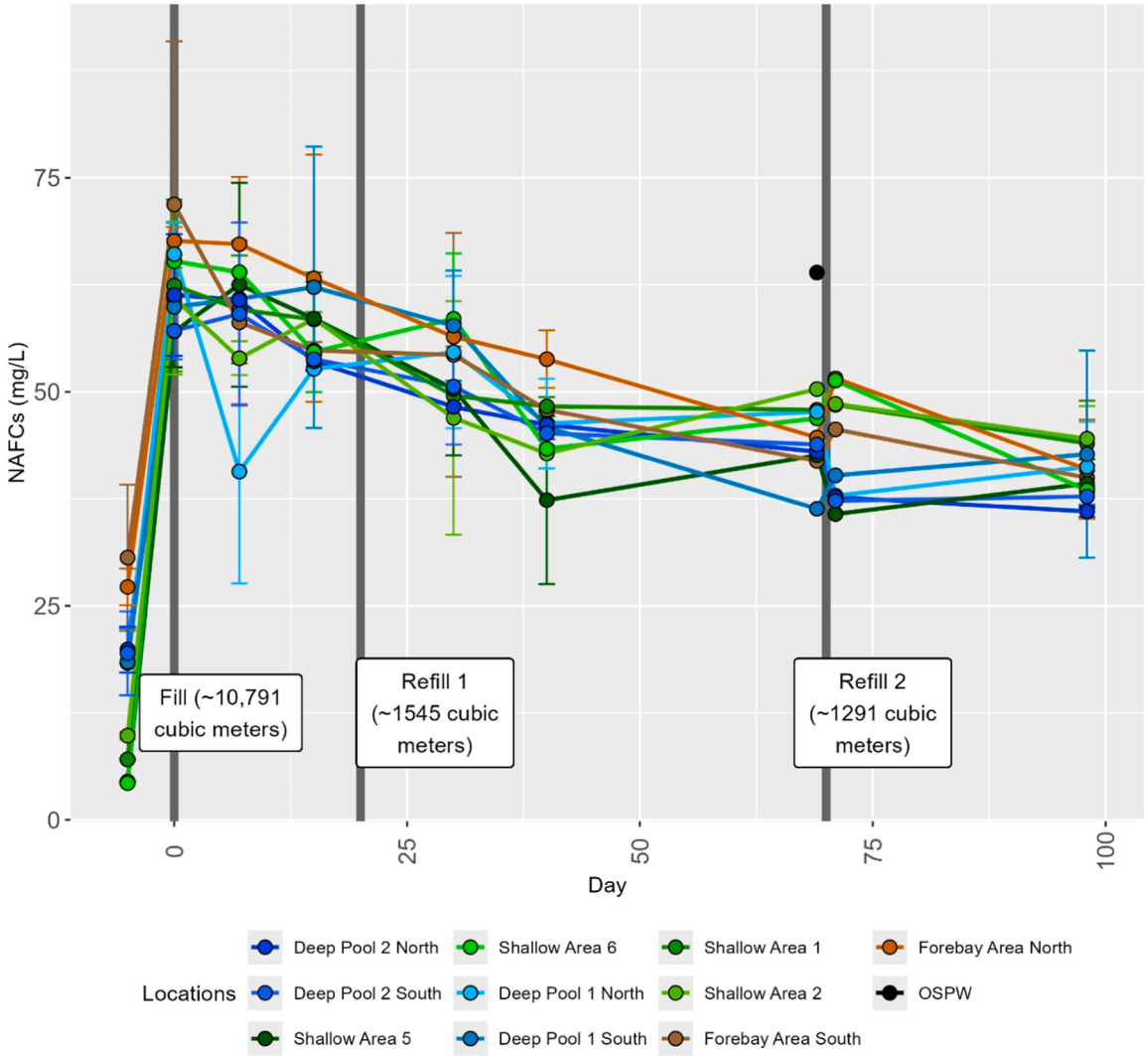

Fig. 3. Concentrations of NAFCs detected in the Kearl constructed wetland treatment system over the 2022 season (after normalization to [Cl^-] to correct for evapotranspiration). Where applicable, dark vertical lines denote wetland fill or refill events, and sample error bars here describe the range of values from duplicate samples at each location, with dots reporting the average value. The initial fill volume of the wetland was approximately 10,791 m of OSPW.

formula types. The trends in heteroatom content were largely consistent with NAFC oxidation (Fig. 4). At the end of the 2021 field season the CWTS was pumped empty of treated OSPW (to the extent this was possible); thus "Winter/Spring Runoff" samples had the greatest overall oxidized-NAFC content as compared to other sampling time points. After the addition of OSPW to the wetland at the beginning of the summer 2022 field season, the wetland NAFC characteristics were similar to those measured in untreated OSPW reference material (Fig. 4). The NAFCs oxidized gradually across the field season, where O_2-NAFCs (i.e., classical NAs) gradually fell from approximately 65 % relative spectral abundance at the beginning of the season to approximately 45 % relative spectral abundance. Added volumes of OSPW (on Days 20 and 70) affected the oxygen-abundance of NAFCs in different ways considering the two different timescales allowed for mixing (i.e., 10 days from Days 20–30, and 1 day from Day 70–71). From Day 15–30, relatively little decrease in O_2-NAFCs is observed, but O_2S-NAFCs do increase in abundance in Shallow Areas, potentially signaling oxidation of neutral sulfur compounds in these segments. From Day 69–71 (i.e., before and after topping-up the CWTS with OSPW, respectively), a disturbance in the uniformity of NAFCs across the wetland is observed, where segments closest to the Forebay (e.g., Shallow Areas 1 & 2) increase in O_2-NAFC abundance, whereas most cells (with the exception of Deep Pool 2 south) are comparable to NAFCs measured on Day 69, which is likely a reflection of the OSPW refill on Day 71. Regardless, throughout the season, consistent with 2021, the O_3- and O_4-NAFCs increased in spectral abundance, consistent with oxidative degradation in the CWTS. Also consistent with 2021, O_3S-NAFCs gradually became undetectable, whereas O_2S-NAFCs remained detectable throughout.

To further investigate the extent to which particular chemical features may have developed or persisted across individual wetland segments, the Orbitrap mass spectral data were also examined using PCA (Fig. 5). Samples of winter/spring run-off were necessarily excluded, as the difference between these samples and all others swamped out the variability of the time series (shown in Figure S3). The time series of the experiment was largely reflected in PCA of the formula abundance data, where the progression was steady, regardless of the two additions of OSPW. There were some effects apparent from these OSPW additions. For example, from days 15–30 (highlighted in Figure S4), the shallow areas separated from other areas of the wetland along the second principal component (PC2), but this effect was short-lived. Further, on day 69 (highlighted in Figure S5) sample data were relatively tightly spaced, where the range along the first principal component (PC1) was ~0.75 units. Post-OSPW refill on day 71, the range of PC1 sample coordinates was ~2.5 units, where wetland segments closest to the CWTS forebay area (e.g., shallow areas 1 & 2) are the furthest to the right along PC1, implying more similarity to the initial (OSPW) state. In contrast, segments geographically further from the forebay (i.e., shallow areas 5 & 6 and deep pool 2 north) shift left along PC1 on day 71, consistent with a greater degree of attenuation, suggesting some mobilization of degraded formulae when the CWTS is re-filled. However, discernible differences largely disappeared by day 98, where wetland sample data are within 1 unit on the far left of the PCA plot, implying relative homogeneity of NAFCs across the wetland.

The PCA showed that the characteristics of NAFCs at Day 0 were

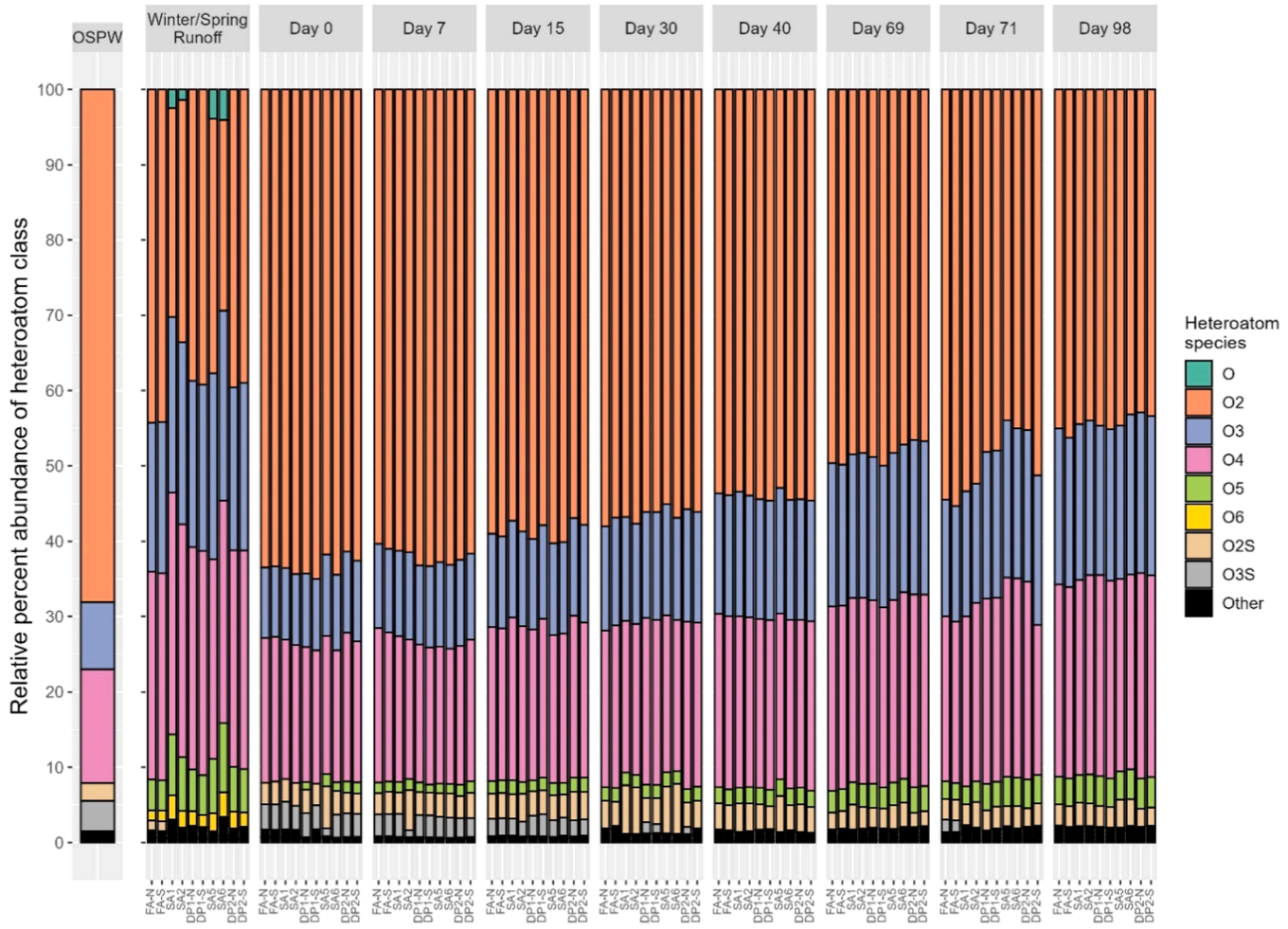

Fig. 4. Percent formula heteroatom (i.e., formula inclusions ignoring carbon and hydrogen) relative spectral abundances of NAFCs detected in the Kearl constructed wetland treatment system over the course of the 2022 field season. Input OSPW values are shown in the left column.

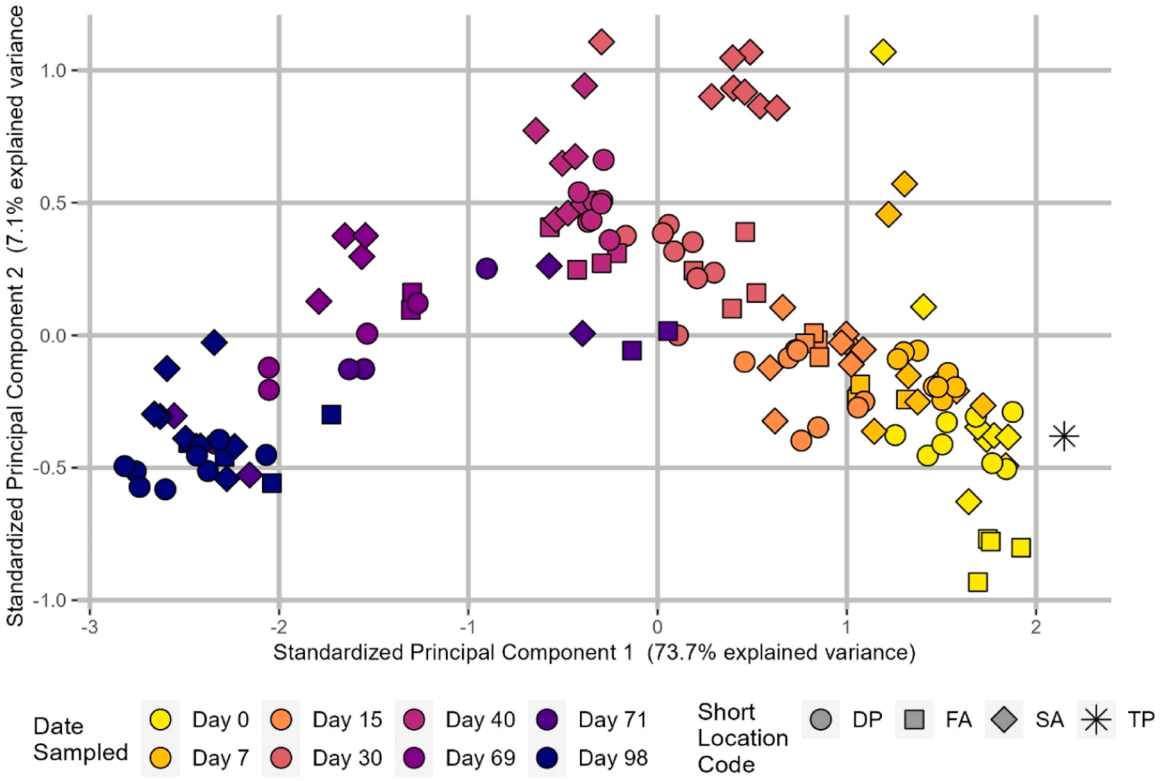

Fig. 5. A principal component analysis of NAFC spectral features detected via Orbitrap mass spectrometry from all CWTS samples taken over the 2022 field season, excluding "Winter/Spring Runoff" samples. Wetland segments included deep pools (DP), the forebay area (FA), shallow areas (SA), and reference tailings pond water (TP; i.e., OSPW).

largely similar across the wetland, and similarly by Day 98 NAFCs were also well-mixed throughout. To summarize changes in spectral features implied by the PCA plot, differences in spectral abundance from Day 0 to Day 98 were calculated, where the relative similarity of the different samples on Days 0 and 98 justified averaging spectral features across pseudo-replicates (i.e., all wetland cells). The results of comparing average spectral features from Day 0 to average spectral features on Day 98 are shown in Fig. 6. Formulae detected on Day 98 are significantly more enriched (by Bonferroni-adjusted Wilcoxon matched pairs signed rank tests) in most O_3- and O_4-NAFCs as compared Day 0, and the highest-#C O_2-NAFCs (#C 16–19) simultaneously decreased across the range of DBE values. However, some formulae were exclusively detected on either Day 0 or Day 98, respectively, and so were not assessed for significance owing to a lack of calculable detection limits for individual formulae during Orbitrap mass spectrometry, but were nonetheless reported. The O_3S-NAFCs had a particular notable decrease in C_{15} to C_{17}/DBE 3–4 formulae that could not be evaluated for significance (owing to a lack of detection on Day 98)).

4. Discussion

Orbitrap mass spectrometry analysis of total NAFCs after CWTS treatment of OSPW in the 2021 and 2022 growing seasons demonstrated NAFC attenuation and oxidation in both seasons. O_2-NAFCs have been specifically implicated as primary toxicants associated with OSPW [35, 47]. Thus, in Fig. 7 we estimated the concentration of O_2-NAFCs as a linear multiple of NAFC concentrations (i.e., Fig. 3) and heteroatom percent spectral abundance (i.e., Fig. 4), as has been previously reported in mesocosm studies [1,56]. By following estimated O_2-NAFC concentrations (Fig. 7) and comparing to the total NAFC attenuation rates (Figure S2), the bulk of decreases in NAFC concentrations is likely due to loss of O_2-NAFCs. The attenuation rate of total NAFCs is -0.53 mg L^{-1} d^{-1} in the initial period between Days 0–15 and 0.25 mg L^{-1} d^{-1} from Days 30–69 (Figure S2). In comparison, estimated attenuation rates of O_2-NAFCs were 0.51 mg L^{-1} d^{-1} from Days 0–15 and 0.19 mg L^{-1} d^{-1} from Days 30–69, and 80 % of the total attenuation rate of all NAFCs from Days 30–69 (Fig. 5). Therefore, most of the attenuation of NAFCs in the CWTS is attributable to decreasing O_2-NAFCs. This demonstrates that the O_2-NAFCs in the OSPW were selectively attenuated by oxidative processes in the CWTS, consistent with previous work [18].

This decrease in attenuation rates might possibly be explained by several factors. For example, decreasing sunlight hours later in the season could lead to decreasing rates of photolysis in surface waters, and similarly affect rates of plant metabolism and chemical uptake. Another explanation may be the possible influence(s) of plant community senescence as growth rates slow and cease towards the end of a season. For example, there is evidence of direct uptake of model NAs by plants [7], which likely slows as plant tissue reaches full height and maturity, and subsequently slow uptake and assimilation of constituents of concern from the water, as has been observed for uptake of nutrients in other treatment wetlands [27]; it is unclear the extent and timing to which autotrophic wetland biota in northern Alberta boreal wetlands might exhibit seasonally similar behaviour of slowing mass gain and potential metabolic processes. Further, if photolysis is a major driver of NAFC attenuation in the CWTS, a combination of decreasing daylight hours and enhanced water surface shading from mature macrophytes could effectively decrease attenuation rates. Apparent slowdowns in NAFC attenuation here may also be partially attributable to mixture dynamics, where more-labile NAFCs may be consumed first, leaving a more recalcitrant residual mixture, which may be interpreted as a decrease in treatment rate. The wetland may also become nutrient-depleted as the season progresses, as oligotrophic organisms become more abundant later on (Beaulieu-Laliberté et al., In prep.). Finally, interpretation of attenuation rates may also be influenced by the quantification method used here, as no internal standard was used to normalize total ionization intensities of samples over time, which could

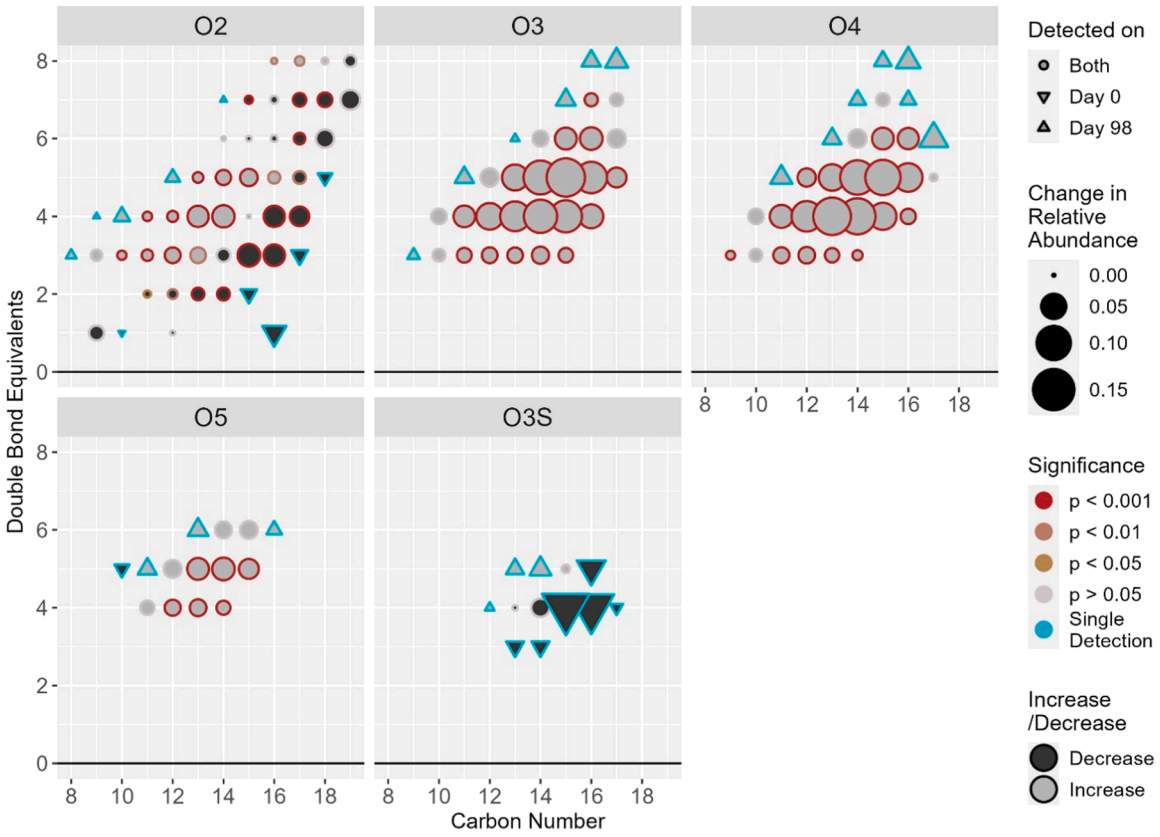

Fig. 6. A carbon number versus double bond equivalents plot summarizing the direction (i.e., increase or decrease) and magnitude of shifts in average spectral features detected across the CWTS from Days 0–98. Data were found to be non-normally distributed and were therefore tested for non-parametric significant differences via Wilcoxon matched pairs signed rank test, where significance is reported using Bonferroni-corrected p-values. Formulae denoted by circles were detected on both Days 0 and 98, whereas triangles denote formulae either detected exclusively on Day 0 (downwards) or Day 98 (upwards).

prevent observation of either increasing or decreasing ionization efficiency with compositional changes (e.g., as are shown in Fig. 4). Temporal changes in NAFC attenuation rates are likely due to a combination of factors, but are at least similar to observations from analogous lab-scale experiments where treatment is initially rapid but subsequently slows [5]. Further investigations are warranted to provide insights on relative weightings of NAFC degradation pathways in the wetland.

It remains unclear how treatment rates in the CWTS were affected by refills of OSPW. The overall influences of OSPW re-fills on NAFCs in the CWTS were examined on different timescales in 2022; the first refill occurred on day 20 (giving 10 days for mixing and attenuation to occur before re-sampling on day 30), whereas the second refill occurred on day 70, giving 1 day for mixing to occur before re-sampling on day 71. The effect of the first re-fill was subtle, as NAFC concentrations were not discernibly affected, as illustrated in Fig. 3. Although concentrations did not increase from Day 20–30, the relative abundance of O_2S-containing compounds increased slightly in the shallow areas by Day 30 post-fill but not in the other wetland segments. In comparison, more readily discernible effects were observed following the second refill on day 70. The effect of the day 70 OSPW refill was apparent in the relative heteroatom abundances shown in Fig. 4, where NAFCs in segments closer to the fill point (e.g., FA-N, FA-S, SA1, SA2) had relatively greater proportions of O_2-NAFCs, whereas later points (with the exception of DP2-S) had O_2, O_3, and O_4-NAFC content more similar to what was observed on day 69. However, the effects of the refill did not persist, as the oxidative trend continued through day 98 of CWTS operation.

With respect to NAFC heteroatom abundances, residual NAFCs (e.g., quantified and characterized winter & spring run-off and residual water) were the most oxygen-rich, potentially owing to a variety of unevaluated factors, such as enhanced dilution of smaller water volumes by local run-off, enhanced photolysis owing to lower water depths, and/or unchecked biodegradation of residual hydrocarbons from the previous field season. This was especially apparent in shallow segments, where oxygen-rich NAFCs (i.e., O_3, O_4, and O_5-NAFCs) were more abundant in winter/spring runoff in shallow areas of the wetland compared to other segments. For the shallow areas (~30 cm depth), the ratio of photo-active versus photo-inactive water volume is high, and so there will likely be photo-induced oxidative radicals [19]. With respect to differentiation of residual NAFCs in winter and spring run-off (e.g., as is shown in Figure S3), shallow areas may also have enhanced snow loading from the presence of aquatic macrophytes trapping snow [25,9]. Further, remains of macrophytes from previous seasons could lower the albedo of these areas, leading to earlier melts and longer open-water periods [13], which would maximize open-water (and therefore treatment) periods in these cells. However, these potential influences have not been specifically evaluated as parameters here, and deserve follow-up study.

The oxidative processes influencing the composition of NAFCs over the 2021 season were generally oxidizing, though drops in concentrations were less readily apparent from Days 15–45. In the 2022 season, NAFC attenuation and oxidation were steady throughout. These processes selectively decreased the abundance of the heaviest O_2-NAFC (e.g., #C 16–19) formulae (Fig. 7), which may help provide an explanation for coinciding decreases in toxicity [15,55], but proving so would require further study. The CWTS also quickly removed some O_3S-NAFCs, providing reason to further target this class of compounds. The NAFCs eventually approached the relative O_2:O_3:O_4 ratios observed in over-wintered residue/run-off samples as concentrations dropped throughout the season. This return to initial conditions is also reflected

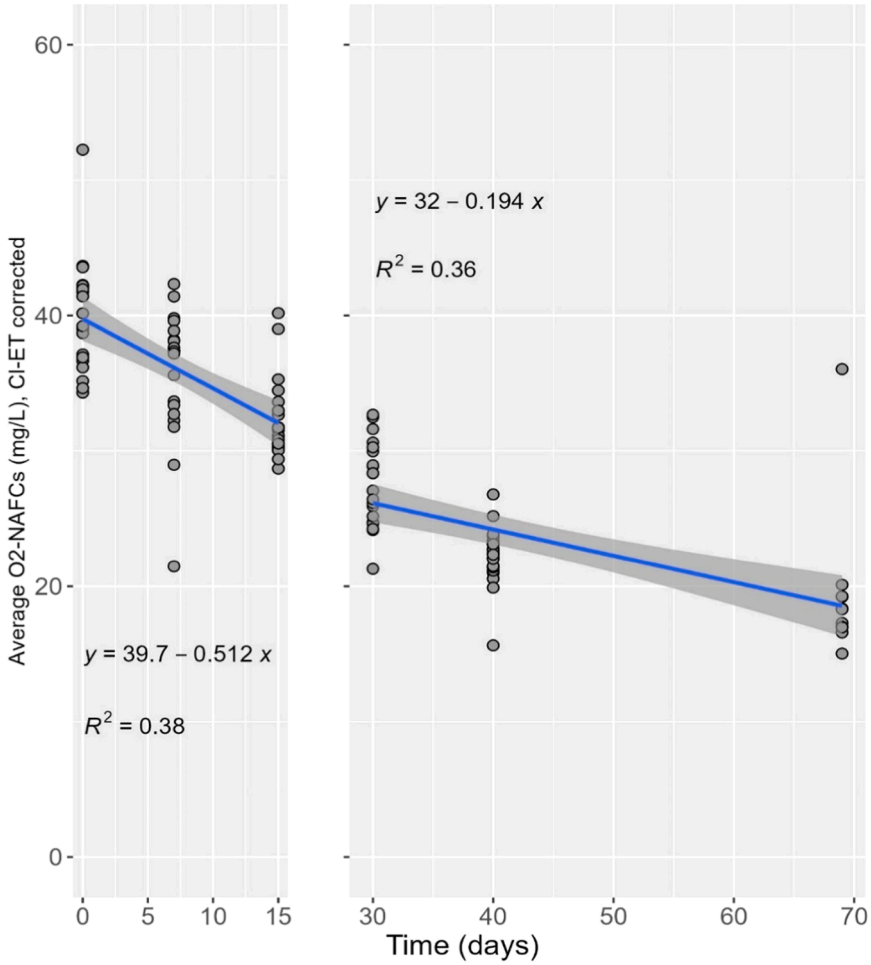

Fig. 7. Linear regressions of estimated O_2-NAFC concentrations in the Kearl constructed wetland treatment system from Days 0–15, and Days 30–69. Quantitative data are split into two periods owing to an addition of fresh OSPW on Day 20 to top-up the volume of water in the wetland to allow for ongoing pumping and circulation.

in water and sediment prokaryote abundance data (Beaulieu-Laliberté et al., In prep.), but the extent to which potential correlations between the microbiology and chemistry might be causative (in either direction) remains unknown.

5. Conclusions

Collectively, this work demonstrates the high efficacy of CWTS for NAFCs in OSPW in Canadian boreal climates. This work provides empirically derived attenuation rates for NAFC attenuation between 0.25 and 0.5 mg L^{-1} d^{-1}, which varies based on seasonal trends. Molecular-level changes in particular NAFCs are consistent with oxidative degradation, which include photolytic and biodegradative processes, but weightings of each cannot be directly inferred from these data. Current studies are providing more insight on the molecular mechanisms associated with NAFC degradation and transformation, including genomics research to better understand the microorganisms and metabolic pathways involved. Work is also ongoing to understand the toxicity reduction in CWTS, as some organisms show reductions in adverse outcomes with CWTS treatment [15]. Further studies may expand investigations for a wider variety of oil sands mine operators, as the effectiveness of these treatments have not yet been evaluated for different OSPW types; or where such tests may have been carried out, data are not publicly available. Future work is encouraged for further CWTS evaluations for OSPW treatment across a wider variety of mine sites, wetland parameterizations, and tailings conditions.

CRediT authorship contribution statement

McMartin Dena: Writing – review & editing, Supervision, Resources, Project administration, Funding acquisition. **John V. Headley:** Writing – review & editing, Validation, Supervision, Resources, Project administration, Methodology, Investigation, Funding acquisition, Formal analysis, Conceptualization. **Ian Vander Meulen:** Writing – review & editing, Writing – original draft, Methodology, Investigation, Formal analysis, Data curation, Conceptualization. **Jason M.E. Ahad:** Writing – review & editing, Methodology, Formal analysis, Conceptualization. **Christine Martineau:** Writing – review & editing, Resources, Methodology, Funding acquisition, Data curation, Conceptualization. **Douglas G. Muench:** Writing – review & editing, Resources, Investigation, Funding acquisition, Data curation, Conceptualization.

Declaration of Competing Interest

The authors declare that they have no known competing financial interests or personal relationships that could have appeared to influence the work reported in this paper

Acknowledgements

The authors acknowledge in-kind support from Imperial Oil Resources Ltd. for access to samples from this project. The authors thank Nuno Fragoso, Paula Reis and Mitchell Alberts for their technical

assistance. Jason Ahad acknowledges research funding from Natural Resources Canada's Environmental Geoscience Program and John Headley acknowledges research funding from Natural Resources Canada through the Office of Energy Research and Development. Douglas Muench and Christine Martineau acknowledge funding support through a Genome Canada Large Scale Applied Research Project (LSARP) grant (#18207) in partnership with Genome Alberta and Genome Quebec. Dena McMartin acknowledges research funding from the Natural Sciences and Engineering Research Council of Canada (#2020-04014).

The authors acknowledge that sampling took place on Treaty 8 territory in the Wood Buffalo region, that sample preparation and Orbitrap mass spectral analyses were conducted on Treaty 6 territory at the National Hydrology Research Center in Saskatoon, and that isotope ratio analyses were carried out both on the traditional territories of the Huron-Wendat people in Québec as well as in the unceded territories of the Mohawk and Algonquin peoples in Ottawa. We acknowledge these traditional territories of these First Nations and Métis peoples and reaffirm our relationships with one another in the spirit of reconciliation.

Appendix A. Supporting information

Supplementary data associated with this article can be found in the online version at doi:10.1016/j.jece.2025.117568.

Data availability

Data will be made available on request.

References

[1] C. Ajaero, K.M. Peru, M. Simair, V. Friesen, G. O'Sullivan, S.A. Hughes, D. W. McMartin, J.V. Headley, Fate and behavior of oil sands naphthenic acids in a pilot-scale treatment wetland as characterized by negative-ion electrospray ionization Orbitrap mass spectrometry, Sci. Total Environ. 631632 (2018) 829–839, https://doi.org/10.1016/j.scitotenv.2018.03.079.
[2] Alberta Energy Regulator, 2022. State of Fluid Tailings Management for Mineable Oil Sands, 2021. Alberta Energy Regulator, Calgary, Alberta.
[3] Alberta Energy Regulator, 2023a. Alberta Energy Outlook 2023 (ST98).
[4] Alberta Energy Regulator, 2023b. State of Fluid Tailings Management for Mineable Oil Sands, 2022. Alberta Energy Regulator, Calgary, Alberta.
[5] M.E. Alberts, R. Hindle, C. Charriere, A.L. Schoonmaker, H. Kaminsky, D. G. Muench, The effect of rhizosphere pH on removal of naphthenic acid fraction compounds from oil sands process-affected water in a willow hydroponic system, Sci. Total Environ. 948 (2024) 174720, https://doi.org/10.1016/j.scitotenv.2024.174720.
[6] M.E. Alberts, I.J. Vander Meulen, D. Degenhardt, K.M. Peru, D.W. McMartin, J. V. Headley, Chemical succession of naphthenic acid fraction compounds in reclamation landscape mesocosms established on centrifuged and co-mixed fluid fine tailings from the Athabasca oil sands, Sci. Total Environ. 957 (2024) 177856, https://doi.org/10.1016/j.scitotenv.2024.177856.
[7] M.E. Alberts, J. Wong, R. Hindle, D. Degenhardt, R. Krygier, R.J. Turner, D. G. Muench, Detection of naphthenic acid uptake into root and shoot tissues indicates a direct role for plants in the remediation of oil sands process-affected water, Sci. Total Environ. 795 (2021) 148857, https://doi.org/10.1016/j.scitotenv.2021.148857.
[8] S.A. Armstrong, J.V. Headley, K.M. Peru, J.J. Germida, Differences in phytotoxicity and dissipation between ionized and nonionized oil sands naphthenic acids in wetland plants, Environ. Toxicol. Chem. 28 (2009) 2167, https://doi.org/10.1897/09-059.1.
[9] J. Assini, K.L. Young, Snow cover and snowmelt of an extensive high arctic wetland: spatial and temporal seasonal patterns, Hydrol. Sci. J. 57 (2012) 738–755, https://doi.org/10.1080/02626667.2012.666853.
[10] A.J. Bartlett, R.A. Frank, P.L. Gillis, J.L. Parrott, J.R. Marentette, L.R. Brown, T. Hooey, R. Vanderveen, R. McInnis, P. Brunswick, D. Shang, J.V. Headley, K. M. Peru, L.M. Hewitt, Toxicity of naphthenic acids to invertebrates: Extracts from oil sands process-affected water versus commercial mixtures, Environ. Pollut. 227 (2017) 271–279, https://doi.org/10.1016/j.envpol.2017.04.056.
[11] A.E. Bauer, L.M. Hewitt, J.L. Parrott, A.J. Bartlett, P.L. Gillis, L.E. Deeth, M. D. Rudy, R. Vanderveen, L. Brown, S.D. Campbell, M.R. Rodrigues, A.J. Farwell, D. G. Dixon, R.A. Frank, The toxicity of organic fractions from aged oil sands process-affected water to aquatic species, Sci. Total Environ. 669 (2019) 702–710, https://doi.org/10.1016/j.scitotenv.2019.03.107.
[12] A.E. Bauer, L.M. Hewitt, J.W. Roy, J.L. Parrott, A.J. Bartlett, P.L. Gillis, W. P. Norwood, M.D. Rudy, S.D. Campbell, M.R. Rodrigues, L.R. Brown, R. Vanderveen, L.E. Deeth, E.A.M. Holman, J. Salerno, J.R. Marentette, C. Lavalle, C. Sullivan, K. Shires, M. Galicia, J. Rubino, M. Brown, A. O'Neill, G. Bickerton, D. G. Dixon, R.A. Frank, The acute toxicity of bitumen-influenced groundwaters from the oil sands region to aquatic organisms, Sci. Total Environ. 848 (2022) 157676, https://doi.org/10.1016/j.scitotenv.2022.157676.
[13] D. Bewley, R. Essery, J. Pomeroy, C. Ménard, Measurements and modelling of snowmelt and turbulent heat fluxes over shrub tundra, Hydrol. Earth Syst. Sci. 14 (2010) 1331–1340, https://doi.org/10.5194/hess-14-1331-2010.
[14] J.A. Brient, P.J. Wessner, Merichem Company, Naphthenic Acids, in: Kirk-Othermer Encyclopedia of Chemical Technology, Wiley Blackwell, United States, 2004, pp. 509–514.
[15] Brueggeman, J., 2023. Application of Biomimetic Extraction to Measure Toxicity of Oil Sands Process-Affected Water to Aquatic Organisms (Master's of Resource Management). Simon Fraser University, Burnaby, British Columbia.
[16] Bull, H., 2021. Evaluation of a Constructed Wetland System for Removal of Metal (loid) Contaminants from Potable Water Treatment Plant Wastewater (MSc). University of Saskatchewan, Saskatoon, SK.
[17] A.M. Cancelli, F.A.P.C. Gobas, Treatment of polycyclic aromatic hydrocarbons in oil sands process-affected water with a surface flow treatment wetland, Environments 7 (2020) 64, https://doi.org/10.3390/environments7090064.
[18] A.M. Cancelli, F.A.P.C. Gobas, Treatment of naphthenic acids in oil sands process-affected waters with a surface flow treatment wetland: mass removal, half-life, and toxicity-reduction, Environ. Res. 213 (2022) 113755, https://doi.org/10.1016/j.envres.2022.113755.
[19] J.K. Challis, A. Parajas, J.C. Anderson, E. Asiedu, J.W. Martin, C.S. Wong, M. S. Ross, Photodegradation of bitumen-derived organics in oil sands process-affected water, Environ. Sci. Process. Impacts 22 (2020) 1243–1255, https://doi.org/10.1039/D0EM00005A.
[20] K.A. Clark, D.S. Pasternack, Hot water separation of bitumen from alberta bituminous sand, Ind. Eng. Chem. 24 (1932) 1410–1416, https://doi.org/10.1021/ie50276a016.
[21] R. Core Team, 2024. R: A language and environment for statistical computing.
[22] D. de Oliveira Livera, T. Leshuk, K.M. Peru, J.V. Headley, F. Gu, Structure-reactivity relationship of naphthenic acids in the photocatalytic degradation process, Chemosphere 200 (2018) 180–190, https://doi.org/10.1016/j.chemosphere.2018.02.049.
[23] J.L. DiMuro, F.M. Guertin, R.K. Helling, J.L. Perkins, S. Romer, A financial and environmental analysis of constructed wetlands for industrial wastewater treatment, J. Ind. Ecol. 18 (2014) 631–640, https://doi.org/10.1111/jiec.12129.
[24] K.D. Duncan, D.R. Letourneau, G.W. Vandergrift, K. Jobst, E. Reiner, C.G. Gill, E. T. Krogh, A semi-quantitative approach for the rapid screening and mass profiling of naphthenic acids directly in contaminated aqueous samples: rapid screening of naphthenic acids, J. Mass Spectrom. 51 (2016) 44–52, https://doi.org/10.1002/jms.3721.
[25] X. Fang, J.W. Pomeroy, Snowmelt runoff sensitivity analysis to drought on the Canadian prairies, Hydrol. Process. 21 (2007) 2594–2609, https://doi.org/10.1002/hyp.6796.
[26] D.L. Gallup, J.A. Curiale, P.C. Smith, Characterization of Sodium Emulsion Soaps Formed from Production Fluids of Kutei Basin, Indonesia, Energy Fuels 21 (2007) 1741–1759, https://doi.org/10.1021/ef060198u.
[27] Z. Ge, C. Feng, X. Wang, J. Zhang, Seasonal applicability of three vegetation constructed floating treatment wetlands for nutrient removal and harvesting strategy in urban stormwater retention ponds, Int. Biodeterior. Biodegrad. 112 (2016) 80–87, https://doi.org/10.1016/j.ibiod.2016.05.007.
[28] Google Earth Pro, 2024.
[29] Government of Canada, 2025. Historical Data - Climate - Environment and Climate Change Canada [WWW Document]. URL ⟨https://climate.weather.gc.ca/historical_data/search_historic_data_e.html⟩ (accessed 1.13.25).
[30] D.M. Grewer, R.F. Young, R.M. Whittal, P.M. Fedorak, Naphthenic acids and other acid-extractables in water samples from Alberta: What is being measured? Sci. Total Environ. 408 (2010) 5997–6010, https://doi.org/10.1016/j.scitotenv.2010.08.013.
[31] M.O. Hagen, E. Garcia-Garcia, A. Oladiran, M. Karpman, S. Mitchell, M.G. El-Din, J.W. Martin, M. Belosevic, The acute and sub-chronic exposures of goldfish to naphthenic acids induce different host defense responses, Aquat. Toxicol. 109 (2012) 143–149, https://doi.org/10.1016/j.aquatox.2011.12.011.
[32] J.V. Headley, K.M. Peru, B. Fahlman, A. Colodey, D.W. McMartin, Selective solvent extraction and characterization of the acid extractable fraction of Athabasca oils sands process waters by Orbitrap mass spectrometry, Int. J. Mass Spectrom. 345347 (2013) 104–108, https://doi.org/10.1016/j.ijms.2012.08.023.
[33] J.V. Headley, K.M. Peru, D.W. McMartin, M. Winkler, Determination of dissolved naphthenic acids in natural waters by using negative-ion electrospray mass spectrometry, J. AOAC Int. 85 (2002) 182–187, https://doi.org/10.1093/jaoac/85.1.182.
[34] R. Hindle, M. Noestheden, K. Peru, J.V. Headley, Quantitative analysis of naphthenic acids in water by liquid chromatography–accurate mass time-of-flight mass spectrometry, J. Chromatogr. A 1286 (2013) 166–174, https://doi.org/10.1016/j.chroma.2013.02.082.
[35] S.A. Hughes, A. Mahaffey, B. Shore, J. Baker, B. Kilgour, C. Brown, K.M. Peru, J. V. Headley, H.C. Bailey, Using ultrahigh-resolution mass spectrometry and toxicity identification techniques to characterize the toxicity of oil sands process-affected water: The case for classical naphthenic acids: TIE of OSPW, Environ. Toxicol. Chem. 36 (2017) 3148–3157, https://doi.org/10.1002/etc.3892.
[36] N.A.S. Hussain, J.L. Stafford, Abiotic and biotic constituents of oil sands process-affected waters, J. Environ. Sci. 127 (2023) 169–186, https://doi.org/10.1016/j.jes.2022.06.012.

[37] G. Ivosev, L. Burton, R. Bonner, Dimensionality reduction and visualization in principal component analysis, Anal. Chem. 80 (2008) 4933–4944, https://doi.org/10.1021/ac800110w.
[38] J.T. Jasper, D.L. Sedlak, Phototransformation of wastewater-derived trace organic contaminants in open-water unit process treatment wetlands, Environ. Sci. Technol. 47 (2013) 10781–10790, https://doi.org/10.1021/es304334w.
[39] T.M.C. Leshuk, Z.W. Young, B. Wilson, Z.Q. Chen, D.A. Smith, G. Lazaris, M. Gopanchuk, S. McLay, C.A. Seelemann, T. Paradis, A. Bekele, R. Guest, H. Massara, T. White, W. Zubot, D.J. Letinski, A.D. Redman, D.G. Allen, F. Gu, A light touch: solar photocatalysis detoxifies oil sands process-affected waters prior to significant treatment of naphthenic acids, acsestwater.3c00616, ACS EST Water (2024), https://doi.org/10.1021/acsestwater.3c00616.
[40] C. Leys, C. Ley, O. Klein, P. Bernard, L. Licata, Detecting outliers: do not use standard deviation around the mean, use absolute deviation around the median, J. Exp. Soc. Psychol. 49 (2013) 764–766, https://doi.org/10.1016/j.jesp.2013.03.013.
[41] C. Li, L. Fu, J. Stafford, M. Belosevic, M. Gamal El-Din, The toxicity of oil sands process-affected water (OSPW): A critical review, Sci. Total Environ. 601602 (2017) 1785–1802, https://doi.org/10.1016/j.scitotenv.2017.06.024.
[42] A. Mahaffey, M. Dubé, Review of the composition and toxicity of oil sands process-affected water, Environ. Rev. 25 (2017) 97–114, https://doi.org/10.1139/er-2015-0060.
[43] D.W. McMartin, J.V. Headley, D.A. Friesen, K.M. Peru, J.A. Gillies, Photolysis of Naphthenic Acids in Natural Surface Water, J. Environ. Sci. Health Part A 39 (2004) 1361–1383, https://doi.org/10.1081/ESE-120037839.
[44] S.A. Messele, P. Chelme-Ayala, M. Gamal El-Din, Catalytic ozonation of naphthenic acids in the presence of carbon-based metal-free catalysts: Performance and kinetic study, Catal. Today 361 (2021) 102–108, https://doi.org/10.1016/j.cattod.2020.01.042.
[45] M.H. Mohamed, I.A. Udoetok, L.D. Wilson, J.V. Headley, Fractionation of carboxylate anions from aqueous solution using chitosan cross-linked sorbent materials, RSC Adv. 5 (2015) 82065–82077, https://doi.org/10.1039/C5RA13981C.
[46] J. Monaghan, D. Steenis, I.J. Vander Meulen, K.M. Peru, J.V. Headley, C.G. Gill, E. T. Krogh, Online membrane sampling for the mass spectrometric analysis of oil sands process affected water-derived naphthenic acids in real-world samples, Separations 10 (2023) 228, https://doi.org/10.3390/separations10040228.
[47] G.D. Morandi, S.B. Wiseman, A. Pereira, R. Mankidy, I.G.M. Gault, J.W. Martin, J. P. Giesy, Effects-directed analysis of dissolved organic compounds in oil sands process-affected water, Environ. Sci. Technol. 49 (2015) 12395–12404, https://doi.org/10.1021/acs.est.5b02586.
[48] Natural Resources Canada, 2020. Photovoltaic Potential and Solar Resource Maps of Canada - Open Government Portal [WWW Document]. URL ⟨https://open.canada.ca/data/en/dataset/8b434ac7-aedb-4698-90df-ba77424a551f⟩ (accessed 1.13.25).
[49] Posit team, 2023. RStudio: Integrated Development Environment for R. Posit Software, PBC, Boston, MA.
[50] V.V. Rogers, K. Liber, M.D. MacKinnon, Isolation and characterization of naphthenic acids from Athabasca oil sands tailings pond water, Chemosphere 48 (2002) 519–527, https://doi.org/10.1016/S0045-6535(02)00133-9.
[51] V.V. Rogers, M. Wickstrom, K. Liber, M.D. MacKinnon, Acute and subchronic mammalian toxicity of naphthenic acids from oil sands tailings, Toxicol. Sci. 66 (2002) 347–355, https://doi.org/10.1093/toxsci/66.2.347.
[52] M.S. Ross, A. dos Santos Pereira, J. Fennell, M. Davies, J. Johnson, L. Sliva, J. W. Martin, Quantitative and qualitative analysis of naphthenic acids in natural waters surrounding the Canadian oil sands industry, Environ. Sci. Technol. 46 (2012) 12796–12805, https://doi.org/10.1021/es303432u.
[53] S. Samanipour, M.J. Reid, J.T. Rundberget, T.K. Frost, K.V. Thomas, Concentration and distribution of naphthenic acids in the produced water from offshore Norwegian North Sea oilfields, Environ. Sci. Technol. 54 (2020) 2707–2714, https://doi.org/10.1021/acs.est.9b05784.
[54] A.G. Scarlett, H.C. Reinardy, T.B. Henry, C.E. West, R.A. Frank, L.M. Hewitt, S. J. Rowland, Acute toxicity of aromatic and non-aromatic fractions of naphthenic acids extracted from oil sands process-affected water to larval zebrafish, Chemosphere 93 (2013) 415–420, https://doi.org/10.1016/j.chemosphere.2013.05.020.
[55] A.G. Scarlett, C.E. West, D. Jones, T.S. Galloway, S.J. Rowland, Predicted toxicity of naphthenic acids present in oil sands process-affected waters to a range of environmental and human endpoints, Sci. Total Environ. 425 (2012) 119–127, https://doi.org/10.1016/j.scitotenv.2012.02.064.
[56] M.C. Simair, J.L. Parrott, M. le Roux, V. Gupta, R.A. Frank, K.M. Peru, C. Ajaero, D. W. McMartin, J.V. Headley, Treatment of oil sands process affected waters by constructed wetlands: evaluation of designs and plant types, Sci. Total Environ. (2021) 145508, https://doi.org/10.1016/j.scitotenv.2021.145508.
[57] M.M. Spacil, J.H. Rodgers, J.W. Castle, W.Y. Chao, Performance of a pilot-scale constructed wetland treatment system for selenium, arsenic, and low-molecular-weight organics in simulated fresh produced water, Environ. Geosci. 18 (2011) 145–156, https://doi.org/10.1306/eg.01281110020.
[58] C. Sun, W. Shotyk, C.W. Cuss, M.W. Donner, J. Fennell, M. Javed, T. Noernberg, M. Poesch, R. Pelletier, N. Sinnatamby, T. Siddique, J.W. Martin, Characterization of naphthenic acids and other dissolved organics in natural water from the Athabasca oil sands region, Canada, Environ. Sci. Technol. 51 (2017) 9524–9532, https://doi.org/10.1021/acs.est.7b02082.
[59] K.E. Trepanier, I.J. Vander Meulen, J.M.E. Ahad, J.V. Headley, D. Degenhardt, Evaluating the attenuation of naphthenic acids in constructed wetland mesocosms planted with Carex aquatilis, Environ. Monit. Assess. 195 (2023) 1228, https://doi.org/10.1007/s10661-023-11776-8.
[60] R.A. van den Berg, H.C. Hoefsloot, J.A. Westerhuis, A.K. Smilde, M.J. van der Werf, Centering, scaling, and transformations: improving the biological information content of metabolomics data, BMC Genom. 7 (2006) 142, https://doi.org/10.1186/1471-2164-7-142.
[61] I.J. Vander Meulen, J.V. Headley, D.W. McMartin, On the occurrence, behaviour, and fate of naphthenic acid fraction compounds in aquatic environments, Sci. Total Environ. 960C (2025) 178383.
[62] I.J. Vander Meulen, D.M. Schock, J.L. Parrott, L.J. Mundy, B.D. Pauli, K.M. Peru, D. W. McMartin, J.V. Headley, Characterization of naphthenic acid fraction compounds in water from Athabasca oil sands wetlands by Orbitrap high-resolution mass spectrometry, Sci. Total Environ. 780 (2021) 146342, https://doi.org/10.1016/j.scitotenv.2021.146342.
[63] Verbeek, A.G., 1995. A toxicity assessment of oil sands wastewater. National Library of Canada = Bibliothèque nationale du Canada, Ottawa.
[64] M.B. Woudneh, M. Coreen Hamilton, J.P. Benskin, G. Wang, P. McEachern, J. R. Cosgrove, A novel derivatization-based liquid chromatography tandem mass spectrometry method for quantitative characterization of naphthenic acid isomer profiles in environmental waters, J. Chromatogr. A 1293 (2013) 36–43, https://doi.org/10.1016/j.chroma.2013.03.040.
[65] Z. Xiaofei, M. Tao, H. Xiaochun, Z. Jinde, W. Xiaoyi, R. Sixian, Flow accelerated naphthenic acid corrosion during high acid crude oil refining, Eng. Fail. Anal. 117 (2020) 104802, https://doi.org/10.1016/j.engfailanal.2020.104802.
[66] L. Yang, A. Bekele, M. Gamal El-Din, Comprehensive characterization of organics in oil sands process water in constructed mesocosms utilizing multiple analytical methods, Environ. Res. 252 (2024) 118972, https://doi.org/10.1016/j.envres.2024.118972.
[67] L. Zhang, Y. Zhang, M. Gamal El-Din, Integrated mild ozonation with biofiltration can effectively enhance the removal of naphthenic acids from hydrocarbon-contaminated water, Sci. Total Environ. 678 (2019) 197–206, https://doi.org/10.1016/j.scitotenv.2019.04.302.
[68] W. Zubot, Z. An, C. Benally, M. Gamal El-Din, Treatment of oil sands process water using petroleum coke: field pilot, J. Environ. Manag. 289 (2021) 112407, https://doi.org/10.1016/j.jenvman.2021.112407.